A thermodynamic model for predicting Ti and Al element of SiO2–Al2O3–FeO–TiO2–CaO–MgO–CaF2 slag in electroslag remelting process

Tan, Jianpeng; Wang, Fang; Liu, Zhongqiu; Baleta, Jakov; Li, Baokuan; Zhang, Beijiang

Download date / Datum preuzimanja: **2025-01-04**

Available online at www.sciencedirect.com

jmr&t
Journal of Materials Research and Technology

Original Article

A thermodynamic model for predicting Ti and Al element of SiO_2−Al_2O_3−FeO−TiO_2−CaO−MgO−CaF_2 slag in electroslag remelting process

Jianpeng Tan [a,b], *Fang Wang* [a,b,*], *Zhongqiu Liu* [b], *Jakov Baleta* [c], *Baokuan Li* [b], *Beijiang Zhang* [d]

[a] *Key Laboratory for Ecological Metallurgy of Multimetallic Ores (Ministry of Education), Northeastern University, Shenyang, 110819 China*
[b] *School of Metallurgy, Northeastern University, Shenyang, 110819 China*
[c] *Faculty of Metallurgy, University of Zagreb, 44 103 Sisak, Croatia*
[d] *High Temperature Materials Research Division, Central Iron & Steel Research Institute, Beijing, 100081 China*

ARTICLE INFO

ABSTRACT

The control of titanium and aluminium in nickel-base superalloy with high titanium and low aluminium during the electroslag remelting (ESR) process has not been resolved well so far. The loss of titanium (Ti) and aluminium (Al) during the ESR process is critical to improve the high-temperature performance of GH4065A superalloy. A thermodynamic model based on the ion and molecule coexistence theory (IMCT) was developed to calculate the Ti and Al content of SiO_2−Al_2O_3−FeO−TiO_2−CaO−MgO−CaF_2 slag system during the ESR process of GH4065A superalloy. Results show that the order of the ability of each element in the slag system to weaken the loss of Al content is in the following order $Al_2O_3 > CaO > CaF_2$, enhance the loss of Al content is $SiO_2 > FeO > TiO_2$, $CaF_2 > MgO$ and enhance the loss of Ti content is $FeO > SiO_2 > Al_2O_3 > CaO$. Considering the influence of the slag system on the elements Al and Ti, the optimal ratio of the slag system is $CaO = 15\ w\%$ $\sim 20\ w\%$, $CaF_2 \geq 60\ w\%$, $Al_2O_3 = 18\ w\% \sim 25\ w\%$, $SiO_2 \leq 0.5\ w\%$, $TiO_2 = 1\ w\% + (0.2\ w\% \sim 0.6\ w\%)$, $MgO \geq 4\ w\%$, $FeO \leq 0.1\ w\%$.

1. Introduction

The combination of vacuum induction melting (VIM), electroslag remelting (ESR), and vacuum arc remelting (VAR) technique are proposed to produce the GH4065A superalloy in recent years. It is well known that the advantage during the ESR process is the cleanness and homogeneity of ingot. However, the Ti and Al element is often oxidized during the ESR process of GH4065A superalloy [1]. The main reason is the chemical reaction between O element in slag and Ti or Al elements in superalloy. There are three reasons explaining this

reaction [2—4]: (1) Self-consuming electrode carries oxygen; (2) Oxidation of slag system is too high; (3) Ti and Al element in GH4065A superalloy are prone to react with unstable oxides in slag system.

The primary approach for decreasing of Ti and Al content in GH4065A superalloy is to reduce the reaction with O elements during the ESR process [5]. The Ti and Al element are distributed unevenly from the top to the bottom of ingot if without appropriate slag. The high-temperature performance of alloy is also weakened accordingly. Therefore, it is crucial to further understand the effect of slag on Ti and Al in superalloy [6].

Some studies [7—9] investigated the effect of slag on the key elements, such as Ti, Si, or Al in the metallurgical process. Chen et al. [10] investigated the titanium loss during the ESR process of A286 and V57 superalloys through experiments method. Pateisky et al. [11] analyzed the reaction of titanium and silicon with the alumina-calcium oxide-fluorspar slags system. They proposed the optimal solutions for reducing the loss of Ti and Si. Park et al. [12] investigated the thermodynamic equilibrium between $CaO-SiO_2-Al_2O_3-MgO-CaF_2$(-$-TiO_x$) slags and the Fe—11mass%Cr melt to understand the thermodynamic behavior of titanium oxide in refining slag. As a critical path to predict the composition content in slag, the ion-molecular coexistence theory (IMCT) method has been developed [13]. Yang et al. [14] developed a thermodynamic model for predicting the phosphate capacity of $CaO-SiO_2$-$-MgO-FeO-Fe_2O_3-MnO-Al_2O_3-P_2O_5$ slag at the steelmaking endpoint during an 80-ton top/bottom combined blown converter steelmaking process based on the IMCT. Duan et al. [15] developed a thermodynamic model to calculate the mass action concentration of ion-coupling agents or structural units in slag based on the IMCT. The developed thermodynamic model for calculating the manganese distribution ratio can determine the respective manganese distribution ratio and capacity of four demanganization products quantitatively. Li et al. [16] predicts the sulfide capacity of $CaO-SiO_2$-$-MgO-Al_2O_3$ ironmaking slag and validated two sets of sulfide capacity data for $CaO-SiO_2-MgO-Al_2O_3$ ironmaking slag based on IMCT. This model can accurately predict the distribution ratio of metallurgical slags. Moreover, several researchers have taken the IMCT method into slag prediction during the ESR process. Yin et al. [17] analyzed the control of aluminum and titanium elements during the electroslag remelting of high titanium and low aluminum alloy Inconel 718. Hou et al. [18] focused on designing appropriate slag for controlling titanium content during 1Cr21Ni5Ti remelting based on the ion and molecule coexistence theory.
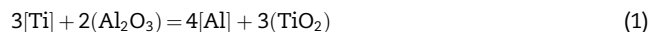
In this paper, a thermodynamic model to calculate the Ti and Al content with $SiO_2-Al_2O_3-FeO-TiO_2-CaO-MgO-CaF_2$ slag system during the ESR process of GH4065A superalloy based on the IMCT is developed. Since the Ti content during the actual ESR process is often loss, the extra TiO_2 of 1 w% will be added in the slag system to keep the Ti content. Moreover, the influence of composition and temperature of the $SiO_2-Al_2O_3-FeO-TiO_2-CaO-MgO-CaF_2$ slag system on the Ti and Al content are analyzed. If the Ti and Al content in industrial ingot could be predicted and controlled, it is beneficial to improve the high-temperature performance of GH4065A superalloy.

2. Thermodynamic model

The chemical composition of GH4065A superalloy is listed in Table 1. During the actual industrial process, the slag system is specific and selected [19]. The slag system used for GH4065A superalloy during the ESR process is shown in Table 2. Moreover, since the Ti content during the ESR process is often reduced significantly, the 1 w% TiO_2 is added to the slag system to lessen the oxidization of titanium.

The reference temperature used in this model are 1873 K, 1923 K, and 1973 K, respectively. In this paper, the decrease of Ti and Al is not only accounted for the oxidation reaction but also the reaction between Ti and FeO or SiO_2 in slag system as follows [14,17,18,20]:

$$3[Ti] + 2(Al_2O_3) = 4[Al] + 3(TiO_2) \tag{1}$$

$$lgK = lg\frac{a_{TiO_2}^3}{a_{Ti}^3 \cdot a_{Al_2O_3}^2} = lg\frac{1}{f_{Ti}^3[Ti]^3} + lg\frac{a_{TiO_2}^3}{a_{Al_2O_3}^2} = -\frac{35300}{T} + 9.94 \tag{2}$$

$$[Ti] + 2(FeO) = (TiO_2) + 2[Fe] \tag{3}$$

$$lgK = lg\frac{a_{TiO_2}}{a_{Ti} \cdot a_{FeO}^2} = lg\frac{1}{f_{Ti}[Ti]^2} + lg\frac{a_{TiO_2}}{a_{FeO}^2} = \frac{34990.6}{T} - 10.49 \tag{4}$$

$$[Ti] + (SiO_2) = (TiO_2) + [Si] \tag{5}$$

$$lgK = lg\frac{a_{TiO_2}}{a_{Ti} \cdot a_{SiO_2}} = lg\frac{1}{f_{Ti}[Ti]^2} + lg\frac{a_{TiO_2}}{a_{FeO}} = \frac{180}{T} + 1.36 \tag{6}$$

The effect of slag system and temperature on Ti oxidation is given as:

$$lg[Ti] = \frac{1}{3}\left\{lg\frac{a_{TiO_2}^3}{a_{Al_2O_3}^2} - 3 lg f_{Ti} - \left(-\frac{35300}{T} + 9.94\right)\right\} \tag{7}$$

$$lg[Ti] = \left\{lg\frac{a_{TiO_2}}{a_{FeO}^2} - lg f_{Ti} - \left(\frac{34990.6}{T} - 10.49\right)\right\} \tag{8}$$

Table 2 — Chemical composition of slag system (w%).

SiO_2	Al_2O_3	FeO	TiO_2	CaO	MgO	CaF_2
0.5	21.2	0.1	0.2	18.0	2.0	58.0

Table 1 — Chemical composition of the GH4065A superalloy (w%).

C	Co	Al	W	Zr	Cr	Mo	Ti	Nb	Ni	B
0.008	13.0	2.13	4.0	0.045	16.0	4.0	3.73	0.7	56.371	0.016

Table 3 − Interaction coefficients e_i^j of the components.

e_i^j	C	Cr	Al	Ti	Mo	Ni
Al	0.091	0.0212	0.0800	0.004	−	−0.0376
Si	−	0.0251 [26]	0.0589 [26]	−	−	−0.0100
Ti	−0.19	0.0250	0.0037	0.0561	0.016	−0.0166

$$\lg[\text{Ti}] = \left\{ \lg\frac{a_{\text{TiO}_2}}{a_{\text{SiO}_2}} - \lg f_{\text{Al}} - \left(\frac{180}{T} + 1.36\right) \right\} \quad (9)$$

When the reaction reaches equilibrium at the slag-metal interface, the content of Ti element in superalloy can be approximated as the sum of Eqs. (2), (4) and (6) shown as:

$$\lg[\text{Ti}] = \frac{1}{3}\left\{ \lg\frac{a_{\text{TiO}_2}^9}{a_{\text{Al}_2\text{O}_3}^2 \cdot a_{\text{FeO}}^6 \cdot a_{\text{SiO}_2}^3} - 3\lg f_{\text{Ti}} - \left(\frac{23403.9}{T} - 5.81\right) \right\} \quad (10)$$

where K denotes the reaction equilibrium constant; $a_{M_xO_y}$ is the activity of the component M_xO_y; T represents the reaction temperature; f_x is the activity coefficient.

$$2\text{Al} + 3\text{FeO} = \text{Al}_2\text{O}_3 + 3\text{Fe} \quad (11)$$

$$\lg K = \lg\frac{a_{\text{Al}_2\text{O}_3}}{a_{\text{Al}}^2 \cdot a_{\text{FeO}}^3} = \lg\frac{1}{f_{\text{Al}}^2 [\text{Al}]^2} + \lg\frac{a_{\text{Al}_2\text{O}_3}^3}{a_{\text{FeO}}^3} = \frac{44383.1}{T} - 11.44 \quad (12)$$

$$4\text{Al} + 3\text{SiO}_2 = 2\text{Al}_2\text{O}_3 + 3\text{Si} \quad (13)$$

$$\lg K = \lg\frac{a_{\text{Al}_2\text{O}_3}^2}{a_{\text{TiO}_2}^3} = \lg\frac{1}{f_{\text{Al}}^4 [\text{Al}]^2} + \lg\frac{a_{\text{Al}_2\text{O}_3}^2}{a_{\text{SiO}_2}^3} = \frac{35840}{T} - 5.86 \quad (14)$$

The effect of slag system and temperature on the Al oxidation is listed:

$$\lg[\text{Al}] = \frac{1}{4}\left\{ \lg\frac{a_{\text{Al}_2\text{O}_3}^2}{a_{\text{TiO}_2}^3} + 4\lg f_{\text{Al}} - \left(-\frac{35300}{T} + 9.94\right) \right\} \quad (15)$$

$$\lg[\text{Al}] = \frac{1}{2}\left\{ \lg\frac{a_{\text{Al}_2\text{O}_3}}{a_{\text{FeO}}^3} - 2\lg f_{\text{Ti}} - \left(\frac{44383.1}{T} - 11.44\right) \right\} \quad (16)$$

$$\lg[\text{Al}] = \frac{1}{4}\left\{ \lg\frac{a_{\text{Al}_2\text{O}_3}^2}{a_{\text{SiO}_2}^3} - 4\lg f_{\text{Al}} - \left(\frac{35840}{T} - 5.86\right) \right\} \quad (17)$$

When a reaction reaches equilibrium at the slag-metal interface, the content of the Al element in superalloy can be approximated as the sum of Eqs. (12), (14) and (15) shown as:

$$\lg[\text{Al}] = \frac{1}{4}\left\{ \lg\frac{a_{\text{Al}_2\text{O}_3}^6}{a_{\text{TiO}_2}^3 \cdot a_{\text{FeO}}^6 \cdot a_{\text{SiO}_2}^3} - 3\lg f_{\text{Al}} - \left(\frac{39976.55}{T} - 9.67\right) \right\} \quad (18)$$

where K indicates the reaction equilibrium constant; $a_{M_xO_y}$ denotes the activity of the component M_xO_y; T is the reaction temperature; f_x is the activity coefficient. Which can be expressed by Eq. (19).

$$\lg f_i = \sum e_i^j \omega_j \quad (19)$$

where ω_j expresses the mass fraction of the component j in the superalloy; f_i denotes the activity coefficient of component i; e_i^j indicates the interaction coefficient between the two components of i and j in the superalloy [21−25], as shown in Table 3.

Based on the IMCT, the remelting slag includes simple ions, simple molecules, and complex molecules, which are in a delicate dynamic equilibrium relationship [27]. The relevant compounds and chemical reactions in the slag are listed in Tables 4 and 5. Since an extra 1w% TiO$_2$ was added to the slag, the mole number of seven components in 101 g slag could be expressed as $c_1 = n_{\text{CaO}}^0$, $c_2 = n_{\text{CaF}_2}^0$, $c_3 = n_{\text{Al}_2\text{O}_3}^0$, $c_4 = n_{\text{SiO}_2}^0$, $c_5 = n_{\text{TiO}_2}^0$, $c_6 = n_{\text{MgO}}^0$, $c_7 = n_{\text{FeO}}^0$. The mass action concentration of components can be calculated as :

$$n_i^0 = \frac{n_i}{\sum n_i} \quad (20)$$

The following equilibrium reaction Eqs. (14)−(21) can be established based on the reaction mass conservation law with IMCT method. Taking Eqs. (13) into ((14−21)), the N_1, N_2, N_3, N_4, N_5, N_6, N_7 after reaction can be calculated and obtained by the Matlab® software.

$$K_{ci} = \exp\left(-\Delta G_i^\theta / RT\right) \quad (21)$$

$$N_1 + N_2 + N_3 + \cdots + N_7 + N_{b1} + N_{b2} + N_{b3} \cdots + N_{b36} = \sum N_i = 1.01 \quad (22)$$

$$c_1 = \begin{pmatrix} 0.5N_1 + N_{b1} + N_{b3} + 2N_{b5} + 3N_{b7} + 12N_{b8} + N_{b9} + N_{b10} + 3N_{b12} + N_{b13} + 3N_{b14} \\ +4N_{b15} + 3N_{b20} + N_{b21} + 2N_{b22} + 3N_{b23} + N_{b24} + 2N_{b25} + 3N_{b26} + N_{b27} + 11N_{b28} \\ +N_{b29} + 3N_{b30} \end{pmatrix} \sum n_i = n_{\text{CaO}}^0 \quad (23)$$

Table 4 – Molar number and mass action concentration in 101 g SiO_2–Al_2O_3–FeO–TiO_2–CaO–MgO–CaF_2 slags based on IMCT [26,28–30].

Item	Structural unit	Symbols	Molar number n_i/mol	Mass action concentration of structural units N_i
Simple ion	$Ca^{2+} + O^{2-}$	1	$n_1 = n_{Ca^{2+},CaO} = n_{O^{2-},CaO}$	$N_1 = \dfrac{n_1}{\sum n_i} = N_{CaO}$
	$Ca^{2+} + 2F^-$	2	$n_2 = n_{Ca^{2+},CaF_2} = 2n_{F^-,CaF_2}$	$N_2 = \dfrac{3n_2}{\sum n_i} = N_{CaF_2}$
	$Mg^{2+} + O^{2-}$	6	$n_6 = n_{Mg^{2+},MgO} = n_{O^{2-},MgO}$	$N_6 = \dfrac{2n_6}{\sum n_i} = N_{MgO}$
	$Fe^{2+} + O^{2-}$	7	$n_7 = n_{Fe^{2+},FeO} = n_{O^{2-},FeO}$	$N_7 = \dfrac{2n_7}{\sum n_i} = N_{FeO}$
Simple and complex molecule	Al_2O_3	3	$n_3 = n_{Al_2O_3}$	$N_3 = \dfrac{n_3}{\sum n_i} = N_{Al_2O_3}$
	SiO_2	4	$n_4 = n_{SiO_2}$	$N_4 = \dfrac{n_4}{\sum n_i} = N_{SiO_2}$
	TiO_2	5	$n_5 = n_{TiO_2}$	$N_5 = \dfrac{n_5}{\sum n_i} = N_{TiO_2}$
	$CaO \cdot SiO_2$	b1	$n_{b1} = n_{CaO \cdot SiO_2}$	$N_{b1} = \dfrac{n_{b1}}{\sum n_i} = N_{CaO \cdot SiO_2}$
	$MgO \cdot SiO_2$	b2	$n_{b2} = n_{MgO \cdot SiO_2}$	$N_{b2} = \dfrac{n_{b2}}{\sum n_i} = N_{MgO \cdot SiO_2}$
	$CaO \cdot Al_2O_3$	b3	$n_{b3} = n_{CaO \cdot Al_2O_3}$	$N_{b3} = \dfrac{n_{b3}}{\sum n_i} = N_{CaO \cdot Al_2O_3}$
	$MgO \cdot Al_2O_3$	b4	$n_{b4} = n_{MgO \cdot Al_2O_3}$	$N_{b4} = \dfrac{n_{b4}}{\sum n_i} = N_{MgO \cdot Al_2O_3}$
	$2CaO \cdot SiO_2$	b5	$n_{b5} = n_{2CaO \cdot SiO_2}$	$N_{b5} = \dfrac{n_{b5}}{\sum n_i} = N_{2CaO \cdot SiO_2}$
	$2MgO \cdot SiO_2$	b6	$n_{b6} = n_{2MgO \cdot SiO_2}$	$N_{b6} = \dfrac{n_{b6}}{\sum n_i} = N_{2MgO \cdot SiO_2}$
	$3CaO \cdot Al_2O_3$	b7	$n_{b7} = n_{3CaO \cdot Al_2O_3}$	$N_{b7} = \dfrac{n_{b7}}{\sum n_i} = N_{3CaO \cdot Al_2O_3}$
	$12CaO \cdot 7Al_2O_3$	b8	$n_{b8} = n_{12CaO \cdot 7Al_2O_3}$	$N_{b8} = \dfrac{n_{b8}}{\sum n_i} = N_{12CaO \cdot 7Al_2O_3}$
	$CaO \cdot 2Al_2O_3$	b9	$n_{b9} = n_{CaO \cdot 2Al_2O_3}$	$N_{b9} = \dfrac{n_{b9}}{\sum n_i} = N_{CaO \cdot 2Al_2O_3}$
	$CaO \cdot 6Al_2O_3$	b10	$n_{b10} = n_{CaO \cdot 6Al_2O_3}$	$N_{b10} = \dfrac{n_{c10}}{\sum n_i} = N_{CaO \cdot 6Al_2O_3}$
	$3Al_2O_3 \cdot 2SiO$	b11	$n_{b11} = n_{3Al_2O_3 \cdot 2SiO_2}$	$N_{b11} = \dfrac{n_{b11}}{\sum n_i} = N_{3Al_2O_3 \cdot 2SiO_2}$
	$3Al_2O_3 \cdot SiO$	b12	$n_{b12} = n_{3Al_2O_3 \cdot SiO_2}$	$N_{b12} = \dfrac{n_{b12}}{\sum n_i} = N_{3Al_2O_3 \cdot SiO_2}$
	$CaO \cdot TiO_2$	b13	$n_{b13} = n_{CaO \cdot TiO_2}$	$N_{b13} = \dfrac{n_{b13}}{\sum n_i} = N_{CaO \cdot TiO_2}$
	$3CaO \cdot 2TiO_2$	b14	$n_{b14} = n_{3CaO \cdot 2TiO_2}$	$N_{b14} = \dfrac{n_{b14}}{\sum n_i} = N_{3CaO \cdot 2TiO_2}$
	$4CaO \cdot 3TiO_2$	b15	$n_{b15} = n_{4CaO \cdot 3TiO_2}$	$N_{b15} = \dfrac{n_{b15}}{\sum n_i} = N_{4CaO \cdot 3TiO_2}$
	$Al_2O_3 \cdot TiO_2$	b16	$n_{b16} = n_{Al_2O_3 \cdot TiO_2}$	$N_{b16} = \dfrac{n_{b16}}{\sum n_i} = N_{Al_2O_3 \cdot TiO_2}$
	$MgO \cdot TiO_2$	b17	$n_{b17} = n_{MgO \cdot TiO_2}$	$N_{b17} = \dfrac{n_{b17}}{\sum n_i} = N_{MgO \cdot TiO_2}$
	$MgO \cdot 2TiO_2$	b18	$n_{b18} = n_{MgO \cdot 2TiO_2}$	$N_{b18} = \dfrac{n_{b18}}{\sum n_i} = N_{MgO \cdot 2TiO_2}$
	$2MgO \cdot TiO_2$	b19	$n_{b19} = n_{2MgO \cdot TiO_2}$	$N_{b19} = \dfrac{n_{b19}}{\sum n_i} = N_{2MgO \cdot TiO_2}$
	$3CaO \cdot 2SiO_2$	b20	$n_{b20} = n_{3CaO \cdot 2SiO_2}$	$N_{b20} = \dfrac{n_{b20}}{\sum n_i} = N_{3CaO \cdot 2SiO_2}$
	$CaO \cdot MgO \cdot 2SiO_2$	b21	$n_{b21} = n_{CaO \cdot MgO \cdot 2SiO_2}$	$N_{b21} = \dfrac{n_{b21}}{\sum n_i} = N_{CaO \cdot MgO \cdot 2SiO_2}$
	$2CaO \cdot MgO \cdot 2SiO_2$	b22	$n_{b22} = n_{2CaO \cdot MgO \cdot 2SiO_2}$	$N_{b22} = \dfrac{n_{b22}}{\sum n_i} = N_{2CaO \cdot MgO \cdot 2SiO_2}$
	$3CaO \cdot MgO \cdot 2SiO_2$	b23	$n_{b23} = n_{3CaO \cdot MgO \cdot 2SiO_2}$	$N_{b23} = \dfrac{n_{b23}}{\sum n_i} = N_{3CaO \cdot MgO \cdot 2SiO_2}$
	$CaO \cdot Al_2O_3 \cdot 2SiO_2$	b24	$n_{b24} = n_{CaO \cdot Al_2O_3 \cdot 2SiO_2}$	$N_{b24} = \dfrac{n_{b24}}{\sum n_i} = N_{CaO \cdot Al_2O_3 \cdot 2SiO_2}$
	$2CaO \cdot Al_2O_3 \cdot SiO_2$	b25	$n_{b25} = n_{2CaO \cdot Al_2O_3 \cdot SiO_2}$	$N_{b25} = \dfrac{n_{b25}}{\sum n_i} = N_{2CaO \cdot Al_2O_3 \cdot SiO_2}$
	$3CaO \cdot 3Al_2O_3 \cdot CaF_2$	b26	$n_{b26} = n_{3CaO \cdot 3Al_2O_3 \cdot CaF_2}$	$N_{b26} = \dfrac{n_{b26}}{\sum n_i} = N_{3CaO \cdot 3Al_2O_3 \cdot CaF_2}$
	$CaO \cdot MgO \cdot SiO_2$	b27	$n_{b27} = n_{CaO \cdot MgO \cdot SiO_2}$	$N_{b27} = \dfrac{n_{b27}}{\sum n_i} = N_{CaO \cdot MgO \cdot SiO_2}$
	$11CaO \cdot 7Al_2O_3 \cdot CaF_2$	b28	$n_{b28} = n_{11CaO \cdot 7Al_2O_3 \cdot CaF_2}$	$N_{b28} = \dfrac{n_{b28}}{\sum n_i} = N_{11CaO \cdot 7Al_2O_3 \cdot CaF_2}$

Table 4 – (continued)

Item	Structural unit	Symbols	Molar number n_i/mol	Mass action concentration of structural units N_i
	$CaO \cdot SiO_2 \cdot TiO_2$	b29	$n_{b29} = n_{CaO \cdot SiO_2 \cdot TiO_2}$	$N_{b29} = \dfrac{n_{b29}}{\sum n_i} = N_{CaO \cdot SiO_2 \cdot TiO_2}$
	$3CaO \cdot 2SiO_2 \cdot CaF_2$	b30	$n_{b30} = n_{3CaO \cdot 2SiO_2 \cdot CaF_2}$	$N_{b30} = \dfrac{n_{b30}}{\sum n_i} = N_{3CaO \cdot 2SiO_2 \cdot CaF_2}$
	$2MgO \cdot 2Al_2O_3 \cdot 5SiO_2$	b31	$n_{b31} = n_{2MgO \cdot 2Al_2O_3 \cdot 5SiO_2}$	$N_{b31} = \dfrac{n_{b31}}{\sum n_i} = N_{2MgO \cdot 2Al_2O_3 \cdot 5SiO_2}$
	$FeO \cdot Al_2O_3$	b32	$n_{b32} = n_{FeO \cdot Al_2O_3}$	$N_{b32} = \dfrac{n_{b32}}{\sum n_i} = N_{FeO \cdot Al_2O_3}$
	$2FeO \cdot SiO_2$	b33	$n_{b33} = n_{2FeO \cdot SiO_2}$	$N_{b33} = \dfrac{n_{b33}}{\sum n_i} = N_{2FeO \cdot SiO_2}$
	$2FeO \cdot TiO_2$	b34	$n_{b34} = n_{2FeO \cdot TiO_2}$	$N_{b34} = \dfrac{n_{b34}}{\sum n_i} = N_{2FeO \cdot TiO_2}$
	$FeO \cdot TiO_2$	b35	$n_{b35} = n_{FeO \cdot TiO_2}$	$N_{b35} = \dfrac{n_{b35}}{\sum n_i} = N_{FeO \cdot TiO_2}$
	$FeO \cdot 2TiO_2$	b36	$n_{b36} = n_{FeO \cdot 2TiO_2}$	$N_{b36} = \dfrac{n_{b36}}{\sum n_i} = N_{FeO \cdot 2TiO_2}$

Table 5 – Chemical reaction equations of possible composite molecules [9,12,14,18,25,27,30–32].

Chemical reaction formula	$\Delta G_i^\theta/(J \cdot mol^{-1})$	Ni
$(Ca^{2+} + O^{2-}) + (SiO_2) = (CaO \cdot SiO_2)$	$-92528 + 2.512T$	$N_{b1} = K_{b1}N_1N_4$
$(Mg^{2+} + O^{2-}) + (SiO_2) = (MgO \cdot SiO_2)$	$23,849 - 29.706T$	$N_{b2} = K_{b2}N_4N_6$
$(Ca^{2+} + O^{2-}) + (Al_2O_3) = (CaO \cdot Al_2O_3)$	$59,413 - 59.413T$	$N_{b3} = K_{b3}N_1N_3$
$(Mg^{2+} + O^{2-}) + (Al_2O_3) = (MgO \cdot Al_2O_3)$	$-18828 - 6.276T$	$N_{b4} = K_{b4}N_3N_6$
$2(Ca^{2+} + O^{2-}) + (SiO_2) = (2CaO \cdot SiO_2)$	$-102090 - 24.267T$	$N_{b5} = K_{b5}N_1^2N_4$
$2(Mg^{2+} + O^{2-}) + (SiO_2) = (2MgO \cdot SiO_2)$	$-56902 - 3.347T$	$N_{b6} = K_{b6}N_4N_6^2$
$3(Ca^{2+} + O^{2-}) + (Al_2O_3) = (3CaO \cdot Al_2O_3)$	$-21757 - 29.288T$	$N_{b7} = K_{b7}N_1^3N_3$
$12(Ca^{2+} + O^{2-}) + 7(Al_2O_3) = (12CaO \cdot 7Al_2O_3)$	$617,977 - 612.119T$	$N_{b8} = K_{b8}N_1^{12}N_3^7$
$(Ca^{2+} + O^{2-}) + 2(Al_2O_3) = (CaO \cdot 2Al_2O_3)$	$-16736 - 25.522T$	$N_{b9} = K_{b9}N_1N_3^2$
$(Ca^{2+} + O^{2-}) + 6(Al_2O_3) = (CaO \cdot 6Al_2O_3)$	$-22594 - 31.798T$	$N_{b10} = K_{b10}N_1N_3^6$
$3(Al_2O_3) + 2(SiO_2) = (3Al_2O_3 \cdot 2SiO)$	$-4354.27 - 10.467T$	$N_{b11} = K_{b11}N_3^3N_4^2$
$3(Al_2O_3) + (SiO_2) = (3CaO \cdot SiO_2)$	$-118,826 - 6.694T$	$N_{b12} = K_{b12}N_1^3N_4$
$(Ca^{2+} + O^{2-}) + (TiO_2) = (CaO \cdot TiO_2)$	$-79900 - 3.35T$	$N_{b13} = K_{b13}N_1N_5$
$3(Ca^{2+} + O^{2-}) + 2(TiO_2) = (3CaO \cdot 2TiO_2)$	$107,100 - 11.35T$	$N_{b14} = K_{b14}N_1^3N_5^2$
$4(Ca^{2+} + O^{2-}) + 3(TiO_2) = (4CaO \cdot 3TiO_2)$	$-292,880 - 17.573T$	$N_{b15} = K_{b15}N_1^4N_5^3$
$(Al_2O_3) + (TiO_2) = (Al_2O_3 \cdot TiO_2)$	$-25270 + 3.924T$	$N_{b16} = K_{b16}N_3N_5$
$(Mg^{2+} + O^{2-}) + (TiO_2) = (MgO \cdot TiO_2)$	$-26400 + 3.14T$	$N_{b17} = K_{b17}N_5N_6$
$(Mg^{2+} + O^{2-}) + 2(TiO_2) = (MgO \cdot 2TiO_2)$	$-27600 + 0.63T$	$N_{b18} = K_{b18}N_5^2N_6$
$2(Mg^{2+} + O^{2-}) + (TiO_2) = (2MgO \cdot TiO_2)$	$-25500 + 1.26T$	$N_{b19} = K_{b19}N_5N_6^2$
$3(Ca^{2+} + O^{2-}) + 2(SiO_2) = (3CaO \cdot 2SiO_2)$	$-236,814 + 9.623T$	$N_{b20} = K_{b20}N_1^3N_4^2$
$(Ca^{2+} + O^{2-}) + (Mg^{2+} + O^{2-}) + 2(SiO_2) = (CaO \cdot MgO \cdot 2SiO_2)$	$-80333 - 51.882T$	$N_{b21} = K_{b21}N_1N_4^2N_6$
$2(Ca^{2+} + O^{2-}) + (Mg^{2+} + O^{2-}) + 2(SiO_2) = (2CaO \cdot MgO \cdot 2SiO_2)$	$-73638 - 63.597T$	$N_{b22} = K_{b22}N_1^2N_4^2N_6$
$3(Ca^{2+} + O^{2-}) + (Mg^{2+} + O^{2-}) + 2(SiO_2) = (3CaO \cdot MgO \cdot 2SiO_2)$	$-205016 - 31.798T$	$N_{b23} = K_{b23}N_1^3N_4^2N_6$
$(Ca^{2+} + O^{2-}) + (Al_2O_3) + 2(SiO_2) = (CaO \cdot Al_2O_3 \cdot 2SiO_2)$	$-4184 - 73.638T$	$N_{b24} = K_{b24}N_1N_3N_4^2$
$2(Ca^{2+} + O^{2-}) + (Al_2O_3) + (SiO_2) = (2CaO \cdot Al_2O_3 \cdot SiO_2)$	$-116,315 - 38.911T$	$N_{b25} = K_{b25}N_1^3N_3N_4$
$3(Ca^{2+} + O^{2-}) + 3(Al_2O_3) + (Ca^{2+} + 2F^-) = (3CaO \cdot 3Al_2O_3 \cdot CaF_2)$	$-44,492 - 73.15T$	$N_{b26} = K_{b26}N_1^2N_2N_3^3$
$(Ca^{2+} + O^{2-}) + (Mg^{2+} + O^{2-}) + (SiO_2) = (CaO \cdot MgO \cdot SiO_2)$	$-124,683 + 3.766T$	$N_{b27} = K_{b27}N_1N_4N_6$
$11(Ca^{2+} + O^{2-}) + 7(Al_2O_3) + (Ca^{2+} + 2F^-) = (11CaO \cdot 7Al_2O_3 \cdot CaF_2)$	$-228,760 - 155.8T$	$N_{b28} = K_{b28}N_1^{11}N_2N_3^7$
$(Ca^{2+} + O^{2-}) + (SiO_2) + (TiO_2) = (CaO \cdot SiO_2 \cdot TiO_2)$	$-114,683 + 7.32T$	$N_{b29} = K_{b29}N_1N_4N_5$
$3(Ca^{2+} + O^{2-}) + 2(SiO_2) + (Ca^{2+} + 2F^-) = (3CaO \cdot 2SiO_2 \cdot CaF_2)$	$-255,180 - 8.2T$	$N_{b30} = K_{b30}N_1^3N_2N_4^2$
$2(Mg^{2+} + O^{2-}) + 2(Al_2O_3) + 5(SiO_2) = (2MgO \cdot 2Al_2O_3 \cdot 5SiO_2)$	$-14422 - 14.808T$	$N_{b31} = K_{b31}N_3^2N_4^5N_6^2$
$(Fe^{2+} + O^{2-}) + (Al_2O_3) = (FeO \cdot Al_2O_3)$	$-59204 + 22.343T$	$N_{b32} = K_{b32}N_3N_7$
$2(Fe^{2+} + O^{2-}) + (SiO_2) = (2FeO \cdot SiO_2)$	$-9395 - 0.227T$	$N_{b33} = K_{b33}N_4N_7^2$
$2(Fe^{2+} + O^{2-}) + (TiO_2) = (2FeO \cdot TiO_2)$	$-33913.08 + 5.86T$	$N_{b34} = K_{b34}N_5N_7^2$
$(Fe^{2+} + O^{2-}) + (TiO_2) = (FeO \cdot TiO_2)$	$68,320 - 43.965T$	$N_{b35} = K_{b32}N_5N_7$
$(Fe^{2+} + O^{2-}) + 2(TiO_2) = (FeO \cdot 2TiO_2)$	-16188.703	$N_{b36} = K_{b36}N_5^2N_7$

$$c_2 = (1/3N_2 + N_{b26} + N_{b28} + 3N_{b30})\sum n_i = n^0_{CaF_2} \qquad (24)$$

$$c_3 = \begin{pmatrix} N_3 + N_{b3} + N_{b4} + N_{b7} + 7N_{b8} + 2N_{b9} + 6N_{b10} + 3N_{b11} \\ + N_{b16} + N_{b24} + N_{b25} + 3N_{b26} + 7N_{b28} + 2N_{b31} + N_{b32} \end{pmatrix}$$
$$\times \sum n_i = n^0_{Al_2O_3} \qquad (25)$$

$$c_4 = \begin{pmatrix} N_4 + N_{b1} + N_{b2} + N_{b5} + N_{b6} + 2N_{b11} + N_{b12} + 2N_{b20} + 2N_{b21} + 2N_{b22} \\ + 2N_{b23} + 2N_{b24} + N_{b25} + N_{b27} + N_{b29} + 2N_{b30} + 5N_{b31} + N_{b33} \end{pmatrix}\sum n_i = n^0_{SiO_2} \qquad (26)$$

$$c_5 = \begin{pmatrix} N_5 + N_{b13} + 2N_{b14} + 3N_{b15} + N_{b16} + N_{b17} + 2N_{b18} + N_{b19} + N_{b29} + N_{b34} \\ + N_{b35} + 2N_{b36} \end{pmatrix}\sum n_i = n^0_{TiO_2} \qquad (27)$$

$$c_6 = \begin{pmatrix} 0.5N_6 + N_{b2} + N_{b4} + 2N_{b6} + N_{b17} + N_{b18} + 2N_{b19} + N_{b21} + N_{b22} \\ + N_{b23} + N_{b27} + 2N_{b31} \end{pmatrix}$$
$$\times \sum n_i = n^0_{MgO} \qquad (28)$$

$$c_7 = (0.5N_7 + N_{b32} + 2N_{b33} + 2N_{b34} + N_{b35} + N_{b36})\sum n_i = n^0_{FeO} \qquad (29)$$

3.   Experimental procedures

In this experiment, the GH4065A alloy and Al_2O_3–TiO_2–CaO–MgO–CaF_2–SiO_2–FeO seven-element slag system are used in the ESR process, respectively. The electrical system of AC mode is carried out with transformer output power 270 kVA, voltage 40.5 V and current 2100 A. The slag samples are proportionally prepared and mixed. Then the prepared slag samples are put into the electric slag furnace, then heated at about 1600 °C for about 5–10 min, finally, cooled at the room temperature. Argon was blown into the furnace. Slag sample was taken from the molten slag after melted for 40 min. In order to investigate the relationship between the titanium and aluminium in ingot, three sets of experiments were done under the same conditions, the experiments are named case1, case2, case3. The Al and Ti in the head and tail of ingot were analyzed, respectively. The chemical composition of slag samples were analysed by the X-ray fluorescence (XRF) technique. The XRF technique were used to analyse the dynamic changes in the content of Al, Ti and other components in slag.

4.   Results and discussion

4.1.   Effect of slag system composition and temperature on Al elememt

The variation of $\lg(a^6_{Al_2O_3}/a^3_{TiO_2}\bullet a^6_{FeO}\bullet a^3_{SiO_2})$ with CaO, CaF$_2$, Al$_2$O$_3$, and MgO content at different temperature are shown in Fig. 1. It can be found the $\lg(a^6_{Al_2O_3}/a^3_{TiO_2}\bullet a^6_{FeO}\bullet a^3_{SiO_2})$ rises with

the increase of CaO, CaF$_2$ and Al$_2$O$_3$ in slag system. In other words, the increase of CaO, CaF$_2$ and Al$_2$O$_3$ in slag will reduce the Al content. It can be deduced that their ability to weaken the loss of Al content is in the following order Al$_2$O$_3$ >- CaO > CaF$_2$. It is obvious that the $\lg(a^6_{Al_2O_3}/a^3_{TiO_2}\bullet a^6_{FeO}\bullet a^3_{SiO_2})$ is almost unchanged when the MgO content increases, which

means that the content of MgO in slag has little effect on the decrease of Al content.

The variation of $\lg(a^6_{Al_2O_3}/a^3_{TiO_2}\bullet a^6_{FeO}\bullet a^3_{SiO_2})$ with SiO$_2$, TiO$_2$, and FeO at different temperature are demonstrated in Fig. 2. It shows that when the content of SiO$_2$, TiO$_2$ and FeO increases, the $\lg(a^6_{Al_2O_3}/a^3_{TiO_2}\bullet a^6_{FeO}\bullet a^3_{SiO_2})$ decreases. Hence, the increase of SiO$_2$, TiO$_2$ and FeO content in slag will cause the decrease of Al content. From the picture, it can be seen that their ability to enhance the loss of Al content is in the following order SiO$_2$ > FeO > TiO$_2$.

The mass action concentration of each element in slag system after the reaction can be calculated by matlab, and then the content of Al elements can be obtained by Eqs. (11)–(17) at different temperature when the slag ratio is different, as shown in Figs. 3 and 4.

It shows the variation of the Al content with CaO content in the slag after the slag-metal interface in an equilibrium state in Fig. 3(a). With the increase of CaO content, the Al content in superalloy also increases. When the CaO content is higher than 15 w%, the Al content in superalloy can be bigger than 2.13 w% when the ESR reaction reaches equilibrium at 1973 K. The CaO can effectively increase the alkalinity of the slag system. Hence, the Al element will not be lost when the CaO content is lower than 15 w%.

Fig. 3(b) represents the variation of Al content with CaF$_2$ content in slag after it reaches equilibrium, the content of Al in superalloy increases with the increase of CaF$_2$ content. Because CaF$_2$ not only effectively lowers the viscosity and melting point of remelted slag, but also greatly improves the fluidity of remelted slag system. When the CaF$_2$ content is greater than 50 w%, the Al content in superalloy can be higher than 2.13 w% when equilibrium at 1973 K. When the CaF$_2$ content is smaller than 50 w%, the Al element in superalloy can be kept at a lower level compared with the other cases.

Fig. 3(c) shows that the variation of Al content with Al$_2$O$_3$ content in slag after the slag-metal interface in an equilibrium state. The Al content tends to influence the melting temperature and viscosity of slag system and also effectively reduce the electrical conductivity of slag system. When the Al$_2$O$_3$
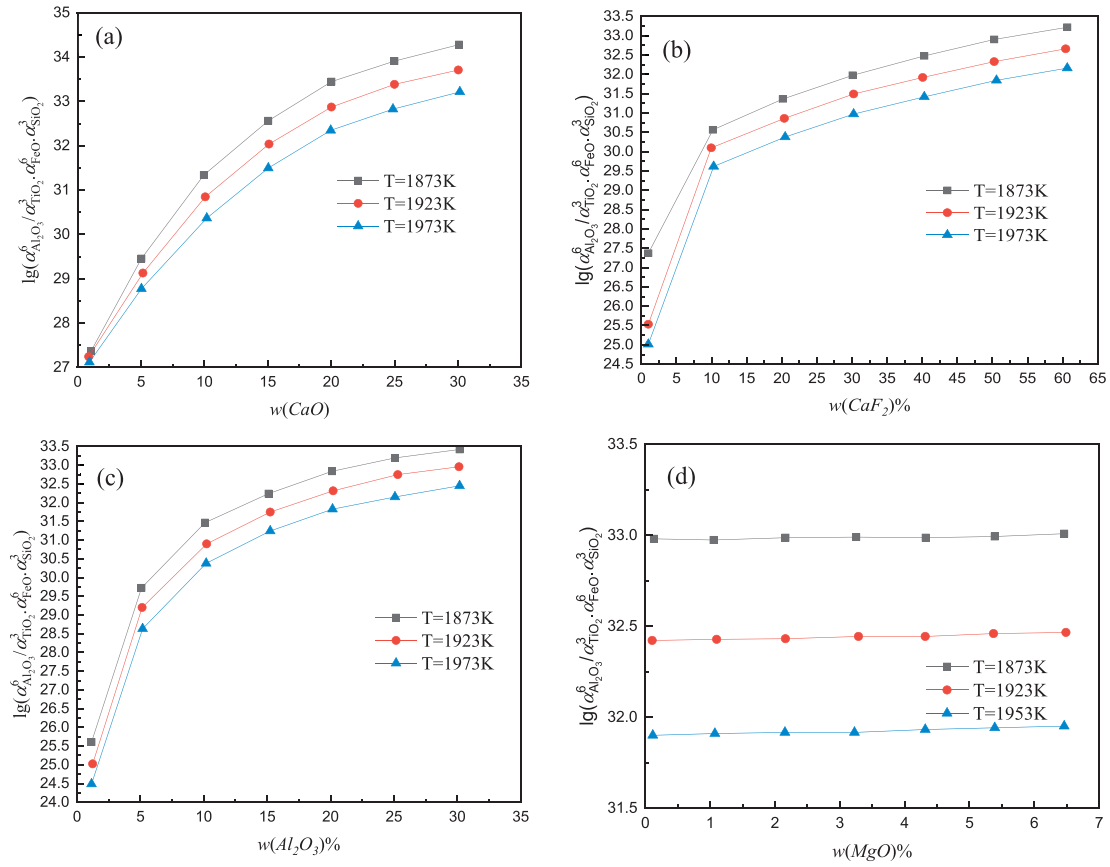
Fig. 1 − **Variation of** $\lg(a^6_{Al_2O_3}/a^3_{TiO_2}\bullet a^6_{FeO}\bullet a^3_{SiO_2})$ **with (a) CaO; (b) CaF₂; (c) Al₂O₃; (d) MgO versus temperature.**
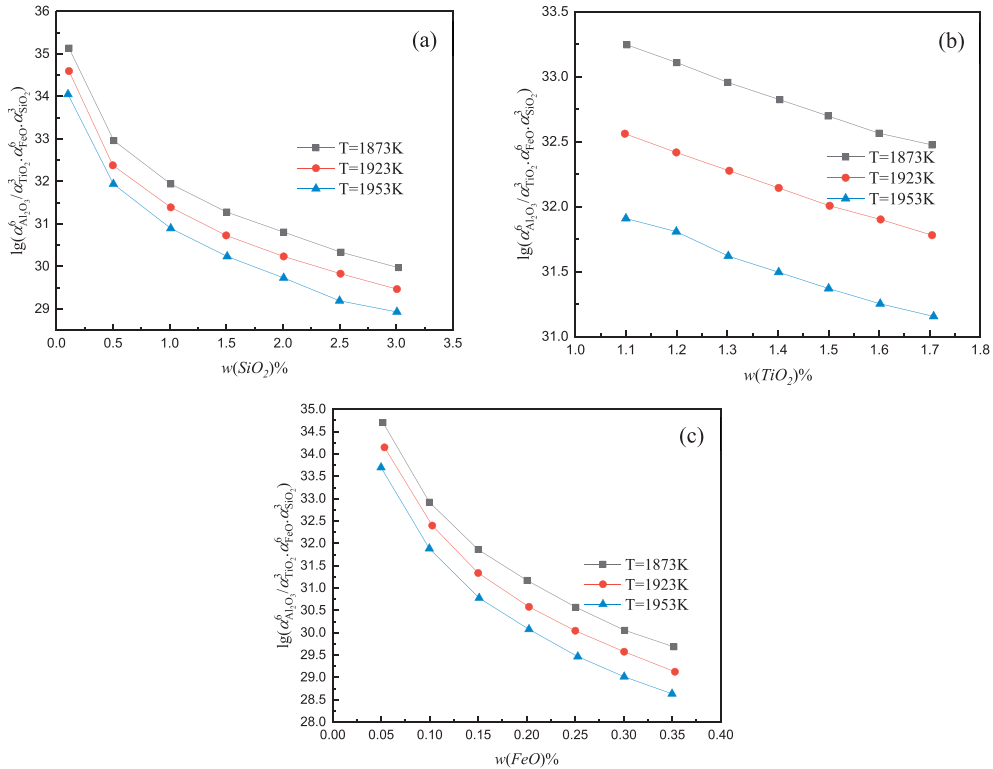
Fig. 2 − **Vgariation of** $\lg(a^6_{Al_2O_3}/a^3_{TiO_2}\bullet a^6_{FeO}\bullet a^3_{SiO_2})$ **with (a) SiO₂; (b) TiO₂; (c) FeO versus temperature.**
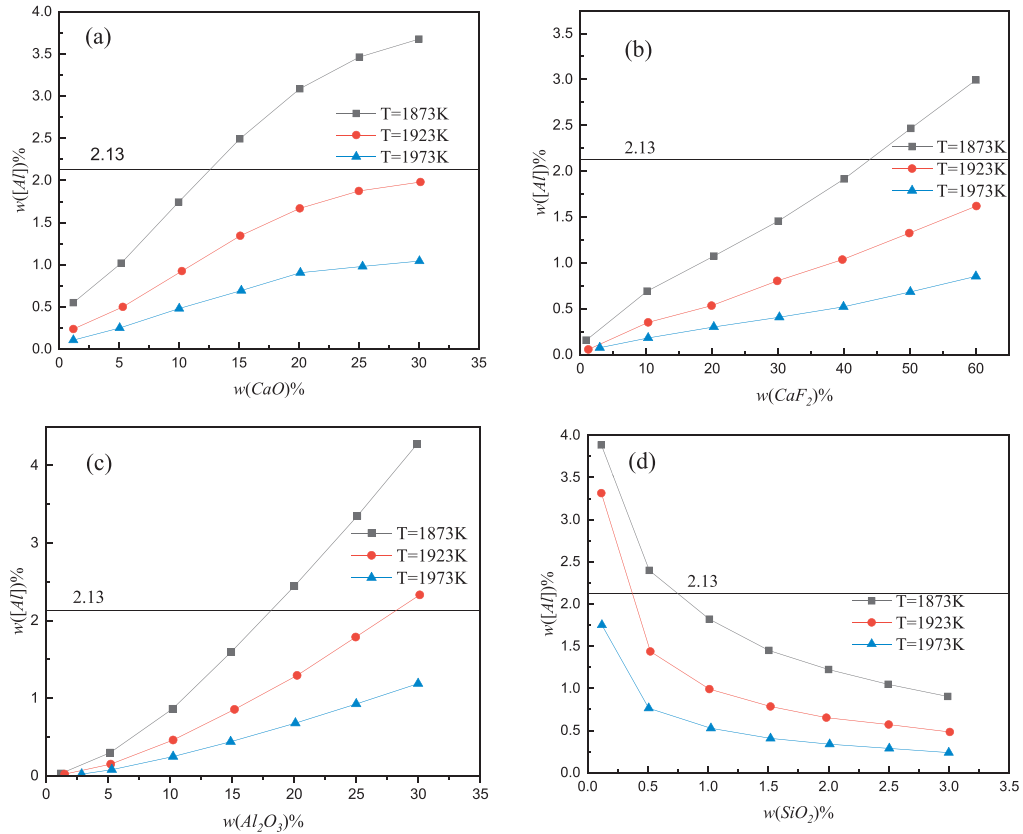
Fig. 3 — Variation of Al content with (a) CaO; (b) CaF$_2$; (c) Al$_2$O$_3$; (d) Si$_2$O$_2$ at 1873 K, 1923 K and 1973 K.
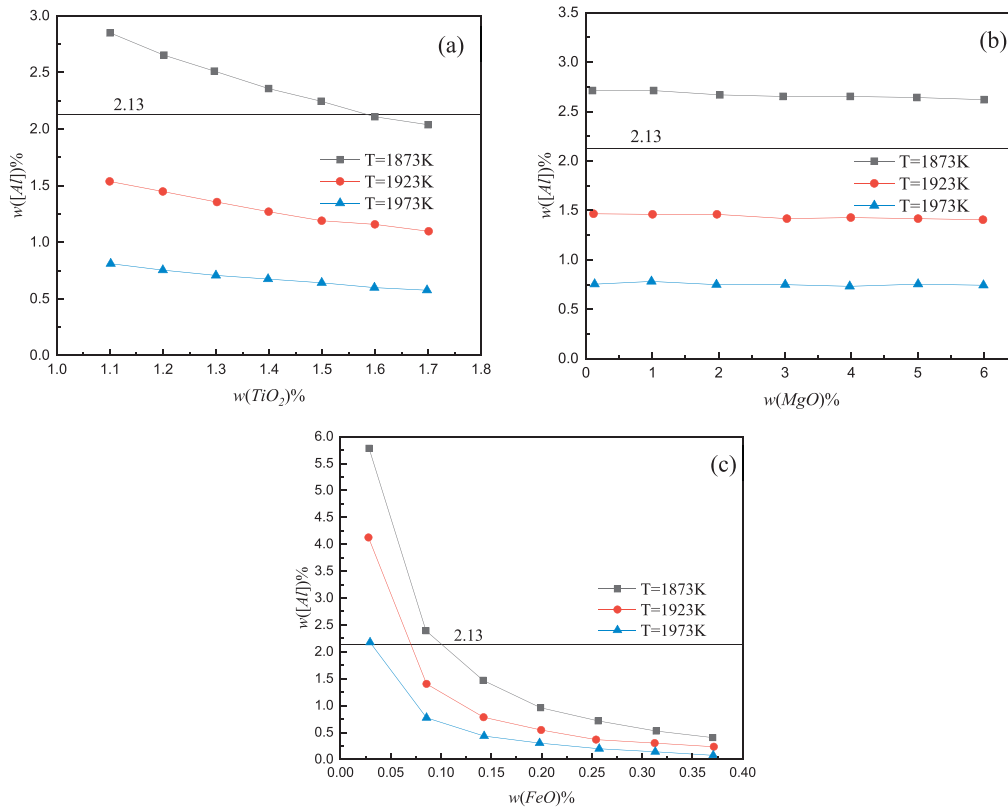

Fig. 4 — Variation of Al content with (a) TiO$_2$; (b) MgO; (c) FeO at 1873 K, 1923 K and 1973 K.

content is greater than 18 w%, the Al content in superalloy can be bigger than 2.13 w% when the ESR reaction reaches equilibrium at 1973 K.

From Fig. 3(d), it depicts that the change of Al content with SiO_2 content in slag when equilibrium. Because it effectively reduces the electrical conductivity and melting temperature of liquid slag system. When the content of SiO_2 is lower than 0.5 w%, the content of Al in superalloy when equilibrium can be less than 2.13 w%.

The change of Al content with TiO_2 content in slag after equilibrium is given in Fig. 4(a). The TiO_2 reacts with the Al in superalloy and then will be oxidized. While the content of TiO_2 is less than 1.6 w%, the Al content in superalloy can be higher than 2.13 w% when equilibrium at 1973 K. While the content of TiO_2 is bigger than 1.6 w%, the decrease of Al content in superalloy can be reduced. Fig. 4(b) describes the change of Al content with MgO content in slag after equilibrium. A thin semi-condensable film at the air-slag interface could be formed by MgO to prevent oxygen caused by slag. In other words, the MgO has little influence on the decrease of Al content. Hence, it is not necessary to pay attention to MgO when considering the decrease of Al content. The change of Al content with FeO content in the slag after equilibrium is shown in Fig. 4(c). As mentioned in Ref. [20], An increase of FeO content promotes the reaction of Eq. (13) to the right, as the FeO content rises, the amount of Al

decreases. With the increase of FeO content, the Al content drops. When the FeO content is lower than 0.12 w%, the Al content in superalloy can be higher than 2.13 w% when equilibrium. When the FeO content is less than 0.12 w%, it can be deduced that the Al content in superalloy will not de decreased.

4.2. Effect of slag system composition and temperature on Ti element

The variation of $\lg(a_{Al_2O_3}^6 / a_{TiO_2}^3 \bullet a_{FeO}^6 \bullet a_{SiO_2}^3)$ with CaO, Al_2O_3, SiO_2, and FeO content at different temperature are shown in Fig. 5. It could be seen that if the content of CaO or Al_2O_3 increases, the $\lg(a_{Al_2O_3}^6 / a_{TiO_2}^3 \bullet a_{FeO}^6 \bullet a_{SiO_2}^3)$ decreases. However, when the content of CaO and Al_2O_3 go up to a certain extent, the $\lg(a_{Al_2O_3}^6 / a_{TiO_2}^3 \bullet a_{FeO}^6 \bullet a_{SiO_2}^3)$ begins to level off and then rise. The reason is that an additional 1 w% TiO_2 into the slag system has a significant effect on the equilibrium of chemical reaction with the change of CaO and Al_2O_3 content. The addition of TiO_2 will drive the direction of reaction with Eqs. (1), (3), and (5) toward the left and reduce the derease of Ti content. If the content of SiO_2 and Al_2O_3 increases, the $\lg(a_{Al_2O_3}^6 / a_{TiO_2}^3 \bullet a_{FeO}^6 \bullet a_{SiO_2}^3)$ always drops. It can be deduced that the ability to enhance the loss of Ti content is in the following order FeO > SiO_2 > Al_2O_3 > CaO.
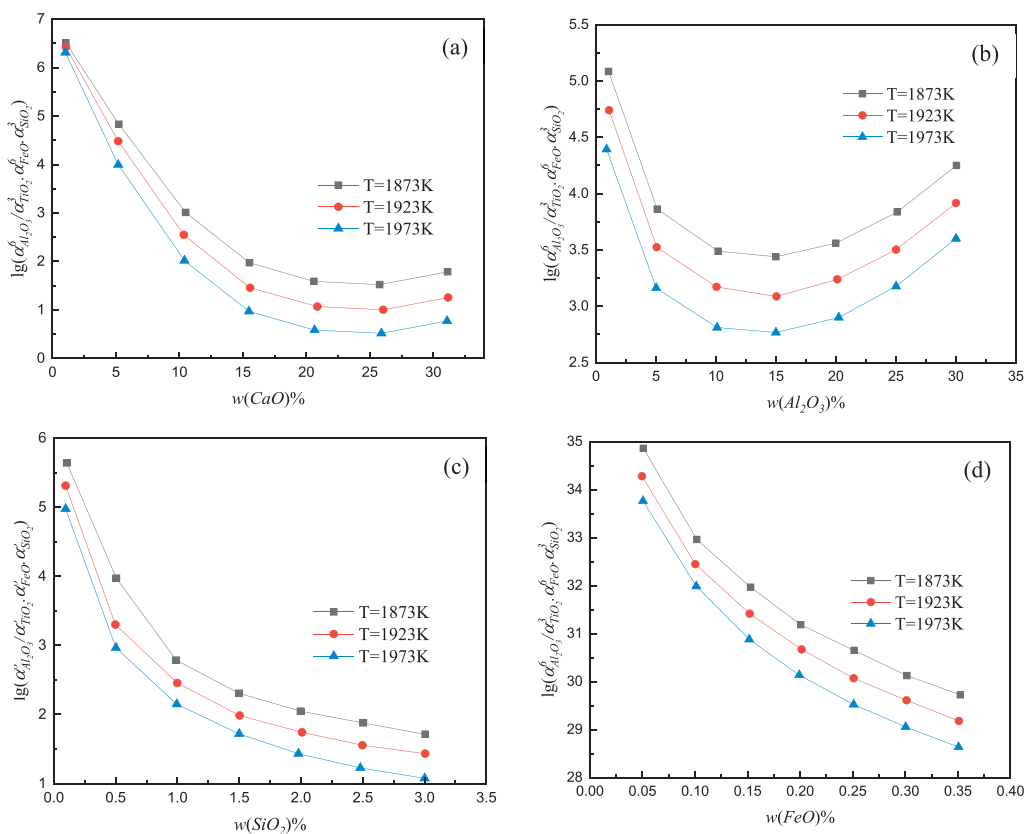

Fig. 5 – **Variation of** $\lg(a_{Al_2O_3}^6 / a_{TiO_2}^3 \bullet a_{FeO}^6 \bullet a_{SiO_2}^3)$ **with composition content of slag versus temperature (a) CaO; (b) Al_2O_3; (c) SiO_2; (d) FeO.**

The variation of $lg(a_{Al_2O_3}^6/a_{TiO_2}^3 \bullet a_{FeO}^6 \bullet a_{SiO_2}^3)$ with CaF$_2$, TiO$_2$, and MgO content at different temperature are demonstrated in Fig. 6. It can be found that the $lg(a_{Al_2O_3}^6/a_{TiO_2}^3 \bullet a_{FeO}^6 \bullet a_{SiO_2}^3)$ rises with the increase of CaF$_2$, TiO$_2$, and MgO content in the slag system. The increase of CaF$_2$, TiO$_2$, and MgO content in slag can reduce Ti content. It can be seen that the ability to weaken the loss of Ti content is in the following order TiO$_2$ > CaF$_2$ > MgO.

As discussed above, the mass action concentration of composition content of slag can be calculated using Matlab software. When the slag composition varies, the content of Ti element versus temperature could be obtained from Eq. (10). The variation of Ti content with CaO content in slag at different temperature is depicted in Fig. 7(a). It could be found that if the CaO content increases, the Ti element in superalloy firstly decreases and then increases. As shown in Table 5, it is proposed that the CaO in slag will form the complex molecules with TiO$_2$, MgO, and SiO$_2$ in slag. Hence, the activity of TiO$_2$ will be weakened, when the CaO content increases. Meanwhile, the content of TiO$_2$ will increase, and the loss of Ti content will decrease. When the CaO content is equal to 16 w%, the chemical reaction is in equilibrium, and the Ti element content in superalloy is close to 3.73 w%. The content of the Ti element cannot be lost if the CaO content is lower than 16 w%. Due to an extra 1%wt TiO$_2$, the chemical reaction will be balanced when the CaO content equals 20 w%. Next, the

reaction will process in the opposite direction. The Ti content will increase again.

Fig. 7 (b) depicts the variation of Ti content with CaF$_2$ content in slag. The CaF$_2$ in slag will form the complex molecules with Al$_2$O$_3$ and CaO in slag is shown in Table 5. Hence, the activity of Al$_2$O$_3$ will be decreased. According to Eq. (1), when the CaF$_2$ content increases, the content of Ti element rises. When the content of CaF$_2$ is greater than 58 w%, the content of Ti element in the superalloy at the reaction temperature of 1973 K can be larger than 3.73 w%. Hence, when the content of CaF$_2$ is larger than 58 w%, it could be prohibited from the loss of Ti content in superalloy.

The change of Ti content with Al$_2$O$_3$ content in slag is demonstrated in Fig. 7(c). The trend of the curve changes from downward to upward. With the increase of Al$_2$O$_3$ content, the Ti element in superalloy decreases first. The Al$_2$O$_3$ in slag and Ti in superalloy will react and give the Al and TiO$_2$ in the slag/metal interface. With the increase of Al$_2$O$_3$ content, the loss of Ti in superalloy improves. The Ti content drops with increasing temperature since the reaction temperature will enhance the loss of Ti content. When the Al$_2$O$_3$ content changes to 15 w%, the chemical reaction is in equilibrium. The content of TiO$_2$ will be the maximum. Later, the chemical reaction will proceed oppositely, and the Ti content will increase again. When the content of Al$_2$O$_3$ is lower than 5 w% and higher than 24 w%, the content of Ti in superalloy is bigger
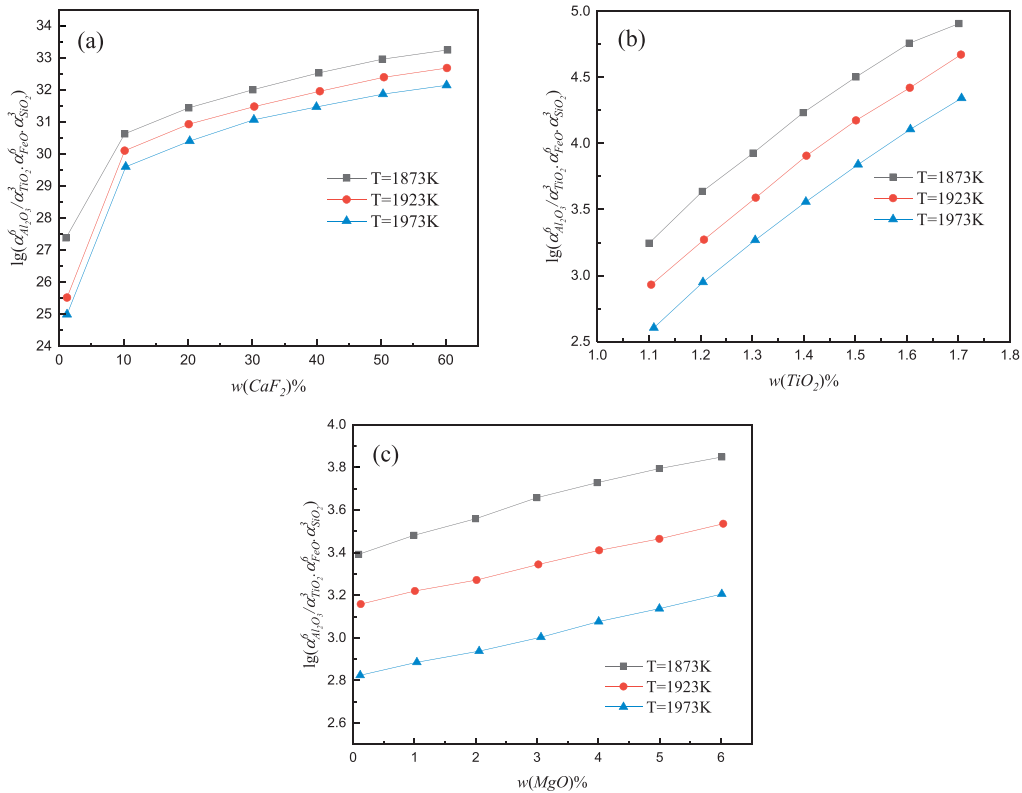

Fig. 6 – Variation of $lg(a_{Al_2O_3}^6/a_{TiO_2}^3 \bullet a_{FeO}^6 \bullet a_{SiO_2}^3)$ with composition content of slag versus temperature (a) CaF$_2$; (b) TiO$_2$; (c) MgO.
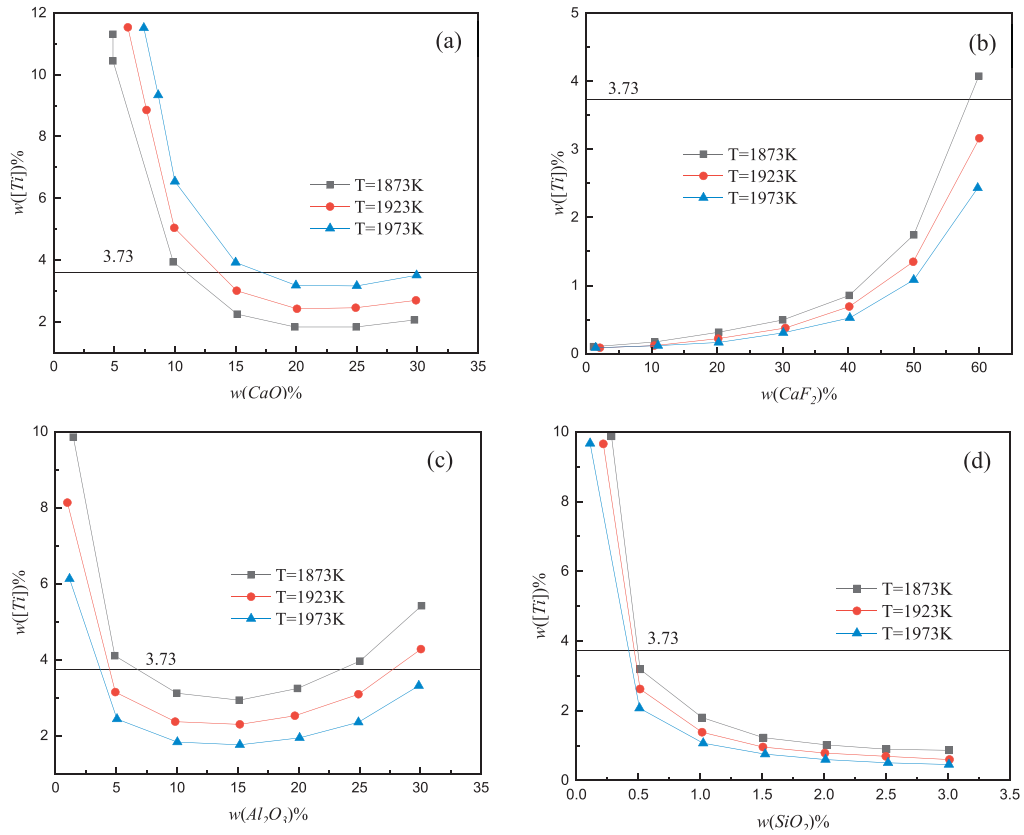
Fig. 7 — **Variation of Ti content with (a) CaO; (b) CaF₂; (c) Al₂O₃; (d) Si₂O₂ at 1873 K, 1923 K and 1973 K.**
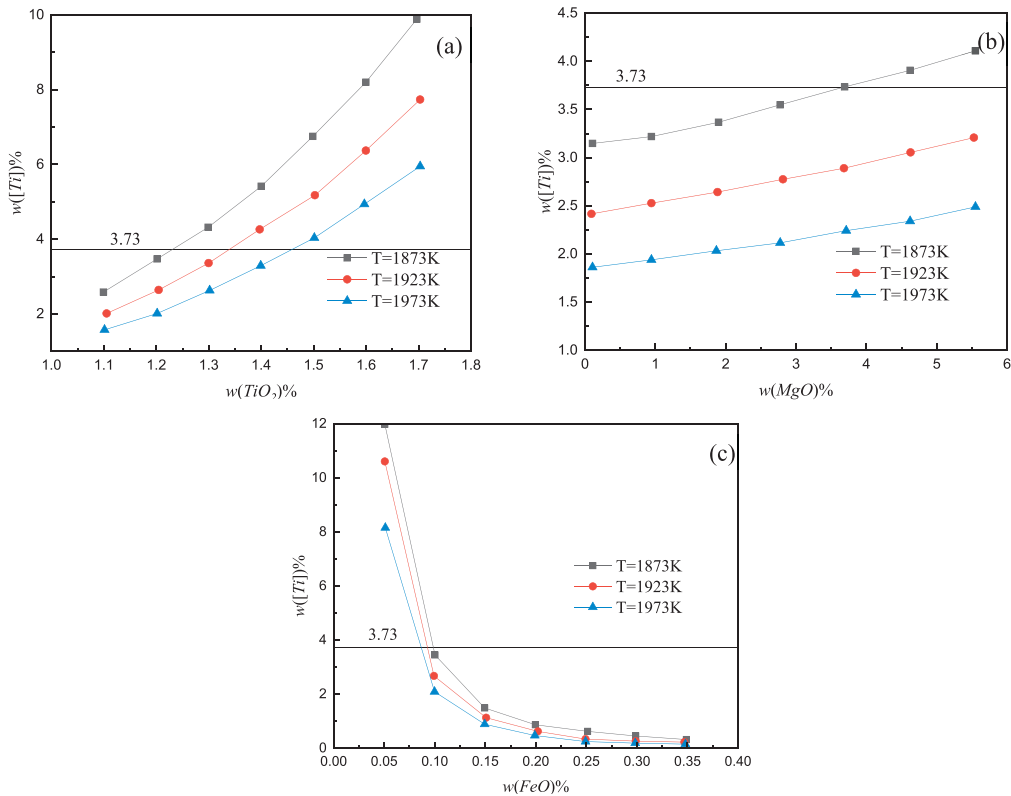

Fig. 8 — **Variation of Ti content with (a) TiO₂; (b) MgO; (c) FeO at 1873 K, 1923 K and 1973 K.**

than 3.73 w%. Compared to the original composition of Al_2O_3 content, the decrease of Ti content can be reduced when the content of Al_2O_3 is higher than 24 w%.The variation of Ti content with SiO_2 content in slag is given in Fig. 7(d). When the SiO_2 content increases, the loss of Ti content will decrease. When the content of SiO_2 is less than 0.5 w%, the content of Ti in superalloy can be much higher than 3.73 w%. In this case, it will not cause the decrease of Ti content in superalloy.

Fig. 8 describes the variation of Ti content with TiO_2, MgO and FeO content in slag. It could be seen that the Ti content in superalloy increases with the increase of TiO_2 content in Fig. 8(a). When the content of TiO_2 in slag is higher, the chemical reaction between the Ti element in superalloy and the unstable oxide in the slag was forced. Hence, the decrease of Ti content is reduced in superalloy. When the content of TiO_2 is higher than 1.2 w%, the Ti element content in superalloy can be larger than 3.73 w%. The Ti content decreases in superalloy can be effectively prevented when the content of TiO_2 is higher than 1.2 w%. The change of Ti content with MgO content in slag is described in Fig. 8(b). The Ti content in superalloy increases with the increase of MgO content. The MgO will enhance the activity of Ti_3O_5 in slag and lessen the activity of TiO_2 in slag. Moreover, the Ti_3O_5 in slag will be decomposed into the TiO_2 in slag and Ti in superalloy [33]. When the content of MgO increases, the decomposition of

Ti_3O_5 in slag will be accelerated, and the Ti content in superalloy will increase. When the content of MgO is greater than 4 w%, the Ti content in superalloy at the reaction equilibrium can be greater than 3.73 w%. Hence, when the content of MgO is higher than 4 w %, the Ti element in superalloy can not be lost. The variation of Ti content with FeO content in slag is represented in Fig. 8(c). The Ti content decreases continuously with the increase of FeO content. It has been pointed out that the activity of TiO_2 decreases significantly with the increasing FeO content in Ref. [30], this is because TiO_2 can be reacted with FeO in the slag to form complex compounds, the formation of complex titanium-containing compounds reduces the effective concentration of TiO_2 in the slag. It has the same trend with our case. When the content of FeO is lower than 0.1 w%, the Ti content in superalloy can be higher than 3.13 w%. When the content of FeO is smaller than 0.1 w%, it will not cause a decrease of Ti content in superalloy.

4.3. Validation of thermodynamic model

In order to further verify the agreement of thermodynamic model and experimental results, Eq. (2) could be changed to Eq. (30), the relationship between $\lg(X_{TiO_2}^3 / X_{Al_2O_3}^2)$ and $\lg([Ti]^3/[Al]^4)$ can be obtained from the experimental results of the slag-metal equilibrium and the model-calculated action concentrations of the slag system components. As shown in Fig. 9, the experimental results are in good agreement with the model calculation.

$$\lg \frac{W_{TiO_2}^3}{W_{Al_2O_3}^2} = -\frac{35300}{T} + 9.94 + \lg \frac{f_{Ti}^3 [Ti]^3}{f_{Al}^4 [Al]^4} - \lg \frac{\gamma_{TiO_2}^3}{\gamma_{Al_2O_3}^4} \qquad (30)$$

$$\gamma_i = N_i / W_i$$

where W_{TiO_2} and $W_{Al_2O_3}$ expresses the mole fraction of TiO_2 and Al_2O_3 in slag, respectively; γ_{TiO_2} and $\gamma_{Al_2O_3}$ denotes the activities coefficients of TiO_2 and Al_2O_3 in slag, respectively.

The contents of Ti and Al at the head and tail in each sample are obtained, and the results of the three sets of experiments are shown in Fig. 10. The experimental value of the average elemental content of Al and Ti at the head and tail of the ingot are in close agreement with the simulated values, indicating that the established thermodynamic model is reasonable.
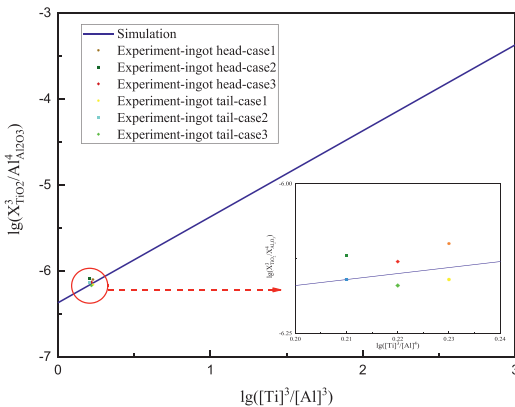

Fig. 9 — Dependence of the $\lg(X_{TiO_2}^3 / X_{Al_2O_3}^2)$ on $\lg([Ti]^3/[Al]^4)$.
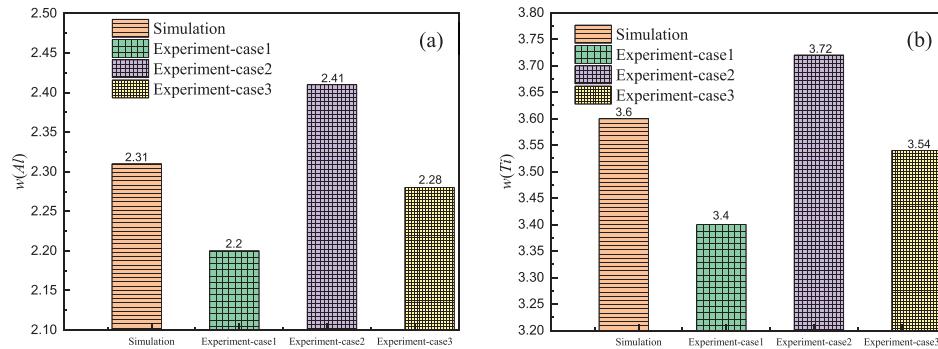

Fig. 10 — Al and Ti content in electroslag ingots with experiment and simulation results.

5.   Conclusions

A thermodynamic model based on IMCT is established to predict the Ti and Al content in the $SiO_2-Al_2O_3-FeO-TiO_2-CaO-MgO-CaF_2$ slag system in the ESR process of GH4065A superalloy. The effect of slag composition on Ti and Al content have been discussed in detail.

(1) Increasing the content of CaF_2 in slag or temperature has a positive effect on reducing the reduction of Al and Ti in the process of electroslag remelting GH4065A alloy; while increasing the content of SiO_2 and FeO in the slag will both increase the loss of Al and Ti elements; while increasing the content of Al_2O_3 and CaO will cause an increase in Al content and a decrease in Ti content of; the effect of MgO on Al is not obvious.

(2) The order of the ability of each element in the slag system to weaken the loss of Al content is in the following order $Al_2O_3 > CaO > CaF_2$, enhance the loss of Al content is $SiO_2 > FeO > TiO_2$, $CaF_2 > MgO$ and enhance the loss of Ti content is $FeO > SiO_2 > Al_2O_3 > CaO$.

(3) Considering the influence of the slag system on the elements Al and Ti, the optimal ratio of the slag system is $CaO = 15\ w\%\sim20\ w\%$, $CaF_2 \geq 60\ w\%$, $Al_2O_3 = 18\ w\%\sim25\ w\%$, $SiO_2 \leq 0.5\ w\%$, $TiO_2 = 1\ w\% + (0.2\ w\% \sim 0.6\ w\%)$, $MgO \geq 4\ w\%$, $FeO \leq 0.1\ w\%$.

Declaration of Competing Interest

The authors declare that they have no known competing financial interests or personal relationships that could have appeared to influence the work reported in this paper.

Acknowledgments

REFERENCES

[1] Hou D, Liu FB, Qu TP, Jiang ZH, Wang DY, Dong YW. Behavior of alloying elements during drawing-ingot-type electroslag remelting of stainless steel containing titanium. ISIJ Int 2018;5:876—85.

[2] Xiang XM, Jiang H, Dong JX, Yao ZH. Thoughts on high performance superalloy design and microstructural characteristics of a newly designed Ni-Cr-Co-W superalloy applied above 850 °C. J Mater Sci Forum 2019;4734:13—24.

[3] Shi CB, Cho JW, Zheng DL, Li J. Fluoride evaporation and crystallization behavior of $CaF_2-CaO-Al_2O_3-(TiO_2)$ slag for electroslag remelting of Ti-containing steels. Int J Min Met Mater 2016;23:627—36.

[4] Li SJ, Cheng GG, Miao ZQ, Che L, Li CW, Jiang XY. Kinetic analysis of aluminum and oxygen variation of G20CrNi2Mo bearing steel during industrial electroslag remelting process. ISIJ Int 2017;57:2148—56.

[5] Wang H, Li J, Shi CB. Evolution of Al_2O_3 inclusions by magnesium treatment in H13 hot work die steel. Ironmak Steelmak 2017;44:128—33.

[6] Thomas A, El-Wahabi M, Cabreran JM, Prado JM. High temperature deformation of Inconel 718. J Mater Process Technol 2006;177:469—72.

[7] Joo Hyun Park, Kyu Yeol Ko. Effect of CaF2 addition on the viscosity and structure of CaO-SiO2-MnO slags. ISIJ Int 2013;53:958—65.

[8] Zhao ZW, Chen XX, Björn Glaser, Yan BJ. Experimental study on the thermodynamics of the CaO-SiO2-Ce2O3 system at 1873 K. Metall Mater Trans B 2019;50:395—406.

[9] Hou D, Jiang ZH, Dong YW, Gong W, Cao YL, Cao HB. Effect of slag composition on the oxidation kinetics of alloying elements during electroslag remelting of stainless steel. ISIJ Int 2017;57:1400—9.

[10] Chen CX, Wang Y, Fu J. A study on the titanium loss during electroslagremelting high titanium and low aluminum content supcralloy. Acta Metall Sin 1981;17:50—7.

[11] Pateisky G. The reaction of titanium and silicon with Al_2O_3-CaO-CaF2 slags in the ESR process. Vac J Sci Technol 1972;9:1318—23.

[12] Park JH, Lee SB, Kim DS, Pak JJ. Thermodynamic of titanium oxide in CaO-SiO2-Al2O3-MgO-CaF2 slag equilibrated with Fe-11mass%Cr melt. ISIJ Int 2009;49:337—42.

[13] Jiang ZH, Hou D, Dong YW, Cao YL, Cao HB, Gong W. Effect of slag on titanium, silicon and aluminum content in superalloy during electroslag remelting. Metall Mater Trans B 2016;47:1465—74.

[14] Yang XM, Shi CB, Zhang M, Zhang DJ. A Thermodynamic model of phosphate capacity for CaO-SiO2-MgO-FeO-Fe2O3-MnO-Al2O3-P2O5 slags equilibrated with molten steel during a top-bottom combined blown converter steelmaking process based on the ion and molecule coexistence theory. Metall Mater Trans B 2011;42:738—70.

[15] Duan SC, Guo XL, Guo HJ, Guo J. A manganese distribution prediction model for $CaO-SiO_2-FeO-MgO-MnO-Al_2O_3$ slags based on IMCT. Ironmak Steelmak 2017;44:168—84.

[16] Li M, Li SS, Ren Y, Yang W, Zhang LF. Modification of inclusions in line pipe steels by Ca-containing ferrosilicon during ladle refining. Ironmak Steelmak 2020;47:6—12.

[17] Yin B, Liu WM, Wang SP, Zheng XM, Yang HC. Thermodynamic analysis of Al and Ti element loss in electroslag remelting Inconel718 superalloy. J Iron Steel Res Int 2019;54:86—94.

[18] Hou D, Jiang ZH, Don YW, Cao H, Gong W. Thermodynamic design of electroslag remelting slag for high titanium and low aluminum stainless stee based on IMCT. Ironmak Steelmak 2016;43:517—25.

[19] Liu ZQ, Niu R, Wu YD, Li BK, Gan Y, Wu M. Physical and numerical simulation of mixed columnar-equiaxed solidification during cold strip feeding in continuous casting. Int J Heat Mass Transfer 2021;173:121237.

[20] Duan SC, Shi X, Wang F, Zhang MC, Sun Y, Guo HJ, et al. A review of methodology development for controlling loss of alloying elements during the electroslag remelting process. J Metall Mater Trans B 2019;50:3055—71.

[21] Park JS, Park JH. Effect of physicochemical properties of slag and flux on the removal rate of oxide inclusion from molten steel. J Metall Mater Trans B 2016;47:3225—30.

[22] Xu RS, Deng SL, Zheng H, Wang W, Song MM, Xu W, et al. Influence of initial iron ore particle size on CO_2 gasification

behavior and strength of ferro-coke. J Iron Steel Res Int 2020;27:875—86.

[23] Hayes RW, Unocic RR, Nasrollahzadeh M. Creep deformation of allvac 718Plus. Metall Mater Trans A 2015;46:218—28.

[24] Ma WB, Liu GQ, Hu BF, Hu PH, Zhang YW. Study of metallic carbide (MC) in a Ni-Co-Cr-based powder metallurgy superalloy. Metall Mater Trans A 2014;45:208—17.

[25] Yang XM, Zhang M, Chai GM, Li JY, Liang Q, Zhang J. Thermodynamic models for predicting dephosphorisation ability and potential of $CaO-FeO-Fe_2O_3-Al_2O_3-P_2O_5$ slags during secondary refining process of molten steel based on ion and molecule coexistence theory. Ironmak Steelmak 2016;43:663—87.

[26] German Iron and Steel Engineers Association. Atlas of slag. 1st ed. China: Metallurgical Industry Press; 1979.

[27] Duan SC, Shi X, Zhang MC, Li B, Yang WS, Wang F, et al. Effect of slag composition on the deoxidation and desulfurization of Inconel 718 superalloy by ESR type slag

without deoxidizer addition. Metall Mater Trans B 2020;51:353—64.

[28] Yang XM, Shi CB. A thermodynamic model for prediction of ironoxide activity in some FeO-containing slag systems. Steel Res Int 2012;83:244—57.

[29] Wang YJ, Ning XJ, Zhang JL, Jiao KX, Wang C. Effect of harmful elements on the coke ratio of blast furnace. J. Ironmak Steelmak 2019;46:253—8.

[30] Liu ZZ, Wu W, Guo XL. SiO2-TiO2-CaO-MgO-FeO-MnO slag system and thermodynamic model of Ti-Si equilibrium in titanium removing process. J Iron Steel Res Int 2013;48:35—49.

[31] Barin J, Knacke O, Kubaschewski. Thermochemical properties of inorganic substances. 1st ed. New York: Springer-Verlag Press; 1977.

[32] Turkdogan ET. Physical chemistry of high temperature technology. 1st ed. New York: Academic Press; 1980.

[33] Su S. Research on control of Ti content in electroslag remelting of R-26. J Iron Steel Res Int 2011;23:282—5.